CHAPTER 37

THE SPIRAL WAVEMAKER FOR LITTORAL DRIFT STUDIES

Robert A. Dalrymple[1] and Robert G. Dean[2]

Abstract

A technique for simulating an infinitely long beach in the laboratory is introduced, with the objective of eliminating end effects usually present with short straight beach sections. The technique involves the spiral wavemaker generating waves in the center of a circular basin.

The wavemaker, consisting of a vertical right-circular cylinder oscillating in a small circle about its axis, is described in detail. Theoretical developments, using small-amplitude wave assumptions, show that the surface wave crests generated by the wavemaker may be described, at a particular time, as an Archimedian-type of spiral, with the wavemaker at its origin. Also, the crests impinge on the circular beach everywhere at the same angle of incidence.

Experiments with a prototype spiral wavemaker verify the theory, with close results for shallow water waves. Littoral drift applications of the wavemaker are given.

Introduction

There have been numerous laboratory studies of littoral drift rates since the first experiments of Krumbein (7) and Saville (8) over 20 years ago. In addition many other model studies have been conducted to determine the effects of groins, jetties and inlets on the adjacent beach. For all of these studies, a short straight beach section has been used, usually with provisions to add sand at the updrift end to simulate infinitely long beaches in nature.

The spiral wavemaker eliminates the end effects present in a straight beach laboratory study by operating in the center of a circular wave basin with a circumferential beach. The waves, which propagate away from the wavemaker in a spiral pattern, impinge on the beach everywhere at the same angle.

In this paper, the linear theory of the spiral wavemaker is presented, along with experimental verification of its validity, and some general results from its use for littoral drift studies.

The Linear Spiral Wavemaker Theory

The theory of wave generation by the spiral wavemaker belongs to a class of water wave problems, which has been extensively investigated, both theoretically and experimentally, particularly for the two-dimensional cases, such as piston and flap wavemaker motions (see, for example, Havelock (6), Ursell, Dean and Yu (9), Biesel and Suquet (1), Galvin (4), and recently Gilbert, Thompson and

---

[1] Graduate Research Associate

[2] Professor, Department of Civil and Coastal Engineering, University of Florida, Gainesville, Florida

Brewer (5)). The case of a vertically-oscillating horizontal cylinder at the water surface has been investigated by Yu and Ursell (10).

The three-dimensional problem of vertical cylinder wavemakers has been examined previously by Havelock (6), who studied the vertical oscillation of an upright cylinder and by Dean (3), for sway (piston) and roll (flap) motion of the cylinder; both of these studies resulted in circular or semi-circular wave crests propagating away from the wavemaker. Recently Black and Mei (2) examined semi-immersed and fully submerged oscillating cylinders in heave, sway and roll. The theory for a pulsating cylindrical wavemaker could also be easily derived. The spiral wavemaker differs from these previous studies by producing waves with an angular dependence that varies with time and distance from the wavemaker.

Assuming an incompressible fluid and irrotational motion, the velocity potential ϕ exists and is governed by the Laplace equation,

$$\nabla^2\phi = \phi_{rr} + \frac{1}{r}\phi_r + \frac{1}{r^2}\phi_{\theta\theta} + \phi_{zz} = 0 \tag{1}$$

in polar coordinates. The subscripts denote partial differentiation. See Figure 1 for the notation. The boundary condition imposed at the bottom is that of no flow through the bottom.

$$-\phi_z = 0 \text{ at } z = -h \tag{2}$$

At the surface, the Cauchy-Poisson condition, which is composed of the linearized dynamic free surface boundary condition ($\eta = \phi_t/g$ at $z = 0$) and the kinematic free surface boundary condition ($-\phi_z = \eta_t$ at $z = 0$), is applied.

$$\phi_z - (\sigma^2/g)\,\phi = 0 \text{ at } z = 0\ , \tag{3}$$

where it has been assumed that the wave motion is periodic in time and of the form $e^{-i\sigma t}$, here $\sigma(= 2\pi/T)$ is the angular frequency. The boundary condition on the cylinder wall ($r = a'$) is determined by assuming that a small perturbation propagates with time around the circumference of the cylinder of radius a, i.e.

$$a' = a + \varepsilon(z) \sin(\theta - \sigma t) \tag{4}$$

where the amplitude of the perturbation $\varepsilon(z)$ may be a function of the elevation, z. The instantaneous radius a' may be rewritten in complex form as

$$a' = a - \varepsilon(z)\, i\, e^{i(\theta - \sigma t)} \tag{5}$$

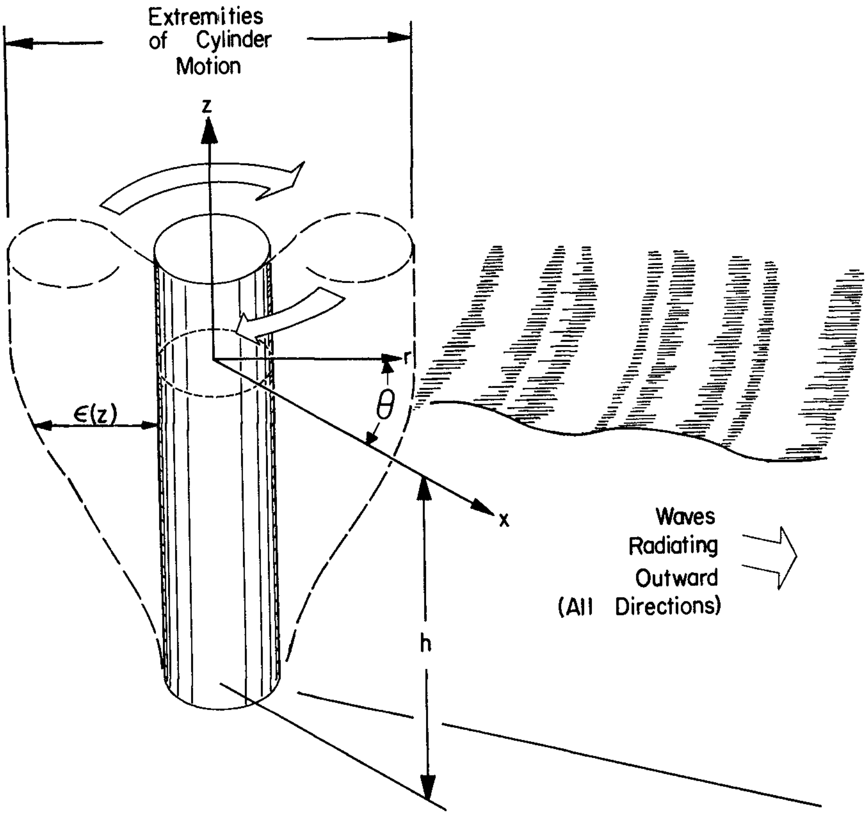

FIGURE 1 SPIRAL WAVEMAKER

The radial velocity, u_r, is

$$u_r = \frac{da'}{dt} = \mathrm{Re}\ \{-\sigma\ \varepsilon\ (z)\ e^{\ i(\theta\ -\ \sigma t)}\} \tag{6}$$

and, under the assumption that $\varepsilon(z)/a << 1$, it is prescribed at the mean position of the cylinder wall, $r = a$.

The final boundary condition to be imposed is that, at $r = \infty$, all waves propagate away from the wavemaker; this is the so-called radiation boundary condition.

The solution of this boundary value problem follows readily from separation of variables. In the z direction, the resulting ordinary differential equation with the two homogeneous boundary conditions is a proper Sturm-Liouville problem and it can be shown that the complete set of eigenfunctions in this coordinate direction is $\{\cosh\ k_o(h + z),\ \cos\ k_m(h+z), m=1,\ 2...\infty\}$, with the relationships

$$\sigma^2 = gk_o\ \tanh\ k_o h \tag{7}$$

$$\sigma^2 = -gk_m\ \tan\ k_m h \tag{8}$$

Here k is a wave number. The subscript zero is used to denote the wave mode associated with the relationship in Eq. 7, and is not to be confused with the customary notation for deep water conditions. The total solution for the velocity potential which gives outward propagating waves is, therefore,

$$\phi(r,\theta,z,t) = A_o\ H_1^{(1)}\ (k_o r)\ \cosh\ \ k_o(h + z)\ e^{i(\theta-\sigma t)}$$

$$+ \sum_{m=1}^{\infty} B_m\ K_1(k_m r)\ \cos\ k_m(h+z)\ e^{i(\theta-\sigma t)} \tag{9}$$

where $H_1^{(1)}(k_o r) = J_1(k_o r) + i\ Y\ (k_o r)$, is the Hankel function of the first kind and $K_1(k_m r)$ is the modified Bessel function of the second kind. The remaining cylinder wall boundary condition (Eq. 6) is used to determine the unknown A_o and the B_m coefficients. Equating the radial velocity of the wall with that determined from the velocity potential, $-\phi_r$, at $r = a$, and using the orthogonality properties of the eigenfunctions in z, A_o and B_m are found to be

$$A_o = \frac{4\sigma\int_{-h}^{0} \varepsilon(z)\ \cosh\ k_o(h+z)dz}{H_1^{(1)\prime}(k_o a)(\sinh\ 2k_o h\ +\ 2k_o h)} \tag{10}$$

$$B_m = \frac{4\sigma\int_{-h}^{0} \varepsilon(z) \cos k_m(h+z)dz}{K_1'(k_m a)(\sin 2k_m h+2k_m h)} \tag{11}$$

where the primes denote differentiation with respect to the arguments. The wave profile, η, is found from the dynamic free surface boundary condition,

$$\eta = \frac{1}{g}\,\phi_t\Big|_{z=0} = R_e\,\{ \frac{-i\sigma A_o}{g}\, H_1^{(1)}(k_o r) \cosh k_o h\, e^{i(\theta-\sigma t)}$$
$$- \sum_{m=1}^{\infty} \frac{i\sigma B_m}{g}\, K_1(k_m r) \cos k_m h\, e^{i(\theta-\sigma t)}\} \tag{12}$$

The waves represented by the summation terms decay rapidly with distance, r, as $K_1(k_m r)/K_1'(k_m a)$ becomes much less than unity with distances of order (h). Thus the waves in the sum in Eq. 12 do not propagate from the cylinder, and only exist near it to provide water motion necessary to match the motion of the cylinder wall.

For two simple types of wavemaker motion, the A_o terms have been evaluated.[1] These are: Case 1, sway, a uniform displacement over depth, analogous to a piston wavemaker motion, and Case 2, a rolling motion with no movement at the bottom, analogous to a flap wavemaker motion.

$$\text{Case 1:} \quad A_o = \frac{4\sigma\,(\frac{S}{2}) \sinh k_o h\, e^{-i\nu}}{k_o\sqrt{J_1'(k_o a)^2 + Y_1'(k_o a)^2}\,(\sinh 2k_o h+2k_o h)} \tag{13}$$

$$\text{Case 2:} \quad A_o = \frac{4\sigma\,(\frac{S}{2})\,(k_o h \sinh k_o h - \cosh k_o h + 1)\, e^{-i\nu}}{k_o^2 h\sqrt{J_1'(k_o a)^2 + Y_1'(k_o a)^2}\,(\sinh 2k_o h+2k_o h)} \tag{14}$$

---

[1] These A_o terms are exactly the same as those derived by Dean (3) for sway and roll motion of the cylinder wavemaker, which generates semicircular waves. His velocity potential was

$$\phi(r,\theta,z,t) = A_o H_1^{(1)}(k_o r)\cosh k_o(h+z) \cos\theta\, e^{-i\sigma t}$$
$$+ \sum_{m=1}^{\infty} B_m K_1(k_m r) \cos k_m(h+z) \cos\theta\, e^{-i\sigma t}$$

The B_m term may be found from Eq.11.

Here $(S/2)$ is the amplitude of the wavemaker displacement $(\varepsilon(0))$ at the surface and the phase, $\nu=\tan^{-1}(Y_1'(k_o a)/J_1'(k_o a))$.

The dimensionless theoretical wave amplitudes, $|\eta|/(S/2)$, have been shown in Figures 2 and 3 for these two cases as a function of $k_o h$ and evaluated at the wavemaker (r=a).

Far from the wavemaker, the wave profile, η, becomes asymptotically

$$\eta = \mathrm{Re}\left\{\frac{-i\sigma A_o}{g}\sqrt{\frac{2}{\pi k_o r}}\cosh k_o h\, e^{i(k_o r+\theta-\sigma t-3\pi/4)}\right\} \quad (15)$$

The asymptotic wave direction, α, that is, the angle between the normal to the wave crest and the radial direction, r, is determined by the gradient of the phase function, $\psi(=k_o r+\theta-\sigma t-3\pi/4-\nu)$ and is expressed as

$$\alpha = \tan^{-1}\left(\frac{1}{k_o r}\right) = \tan^{-1}(L_o/2\pi r) \quad (16)$$

This relationship is shown in Figure 4. It should be noted that, in the limit as $r\to\infty$, the wave direction is not a function of the size of the wavemaker, being solely a function of the period of and distance from the wave maker and the water depth. Also the direction of the wave tends to be more radial with increasing distance. The pattern of the wave crest is found by setting the phase function equal to a constant, say $\pi/2$. Rearranging, the following equation of the form of an Archimedian spiral results.

$$r = \frac{1}{k_o}(5\pi/4 - \theta + \sigma t + \nu) \quad (17)$$

The power necessary to produce the propagating waves is easily found by two means. (Note that theoretically the standing waves require no energy after they have been initially established). The first is to integrate the dynamic pressure dotted with u_r, the radial velocity, over the wetted surface of the cylinder, and then taking the time average,

$$P = \overline{\int_0^{2\pi}\int_{-h}^{0} -\rho g\, \phi_t\, \phi_r\, dz\; a\, d\theta} \quad (18)$$

where Bernoulli's equation has been used, or by equating the power to the averaged energy flux of the propagating wave far from the cylinder, say, at r = b,

$$P = \overline{\int_0^{2\pi} \frac{\rho g|\eta|^2}{2} C_g\, b\, d\theta} \quad (19)$$

where C_g is the group velocity of the waves.

$$C_g = \frac{\sigma}{2k_o}\left(1 + \frac{2k_o h}{\sinh 2k_o h}\right) \quad (20)$$

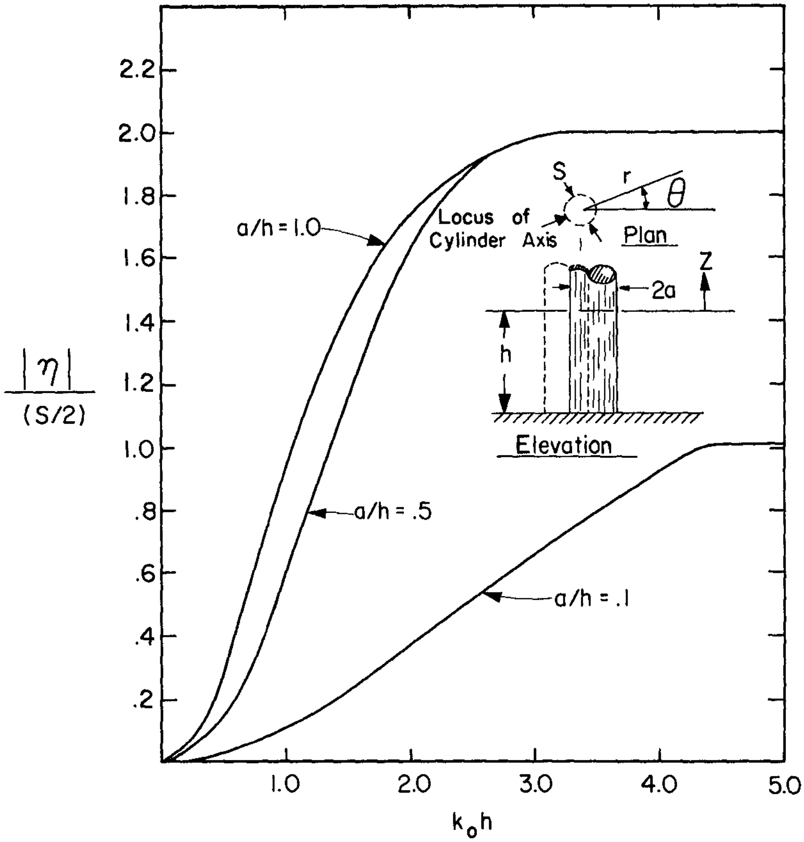

FIGURE 2 DIMENSIONLESS PROGRESSIVE WAVE AMPLITUDE EVALUATED AT CYLINDER, CASE I

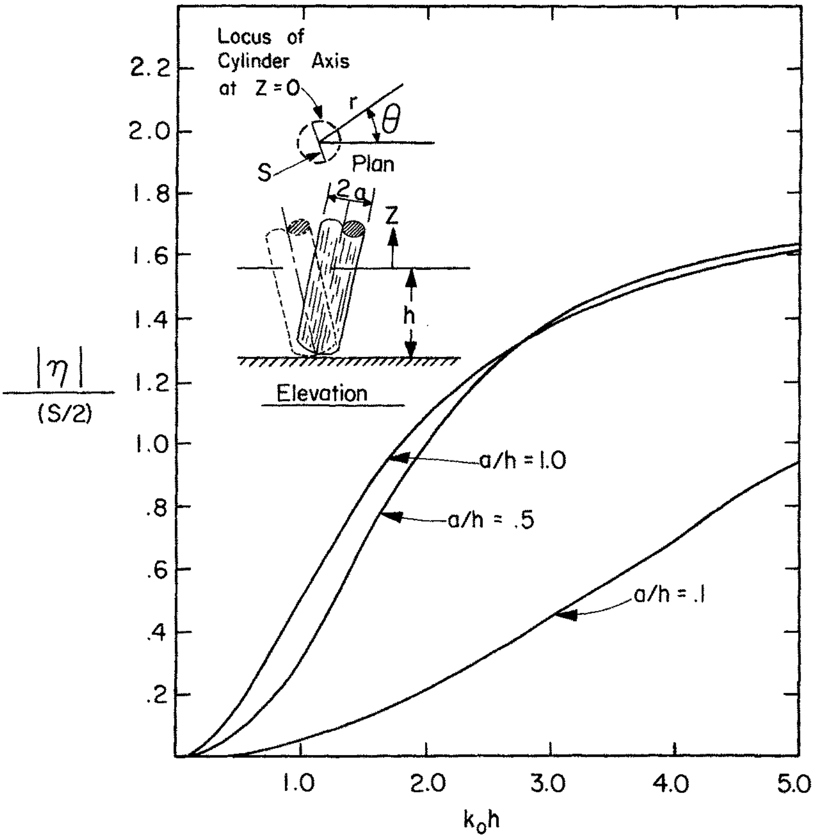

FIGURE 3 DIMENSIONLESS PROGRESSIVE WAVE AMPLITUDE EVALUATED AT CYLINDER, CASE 2

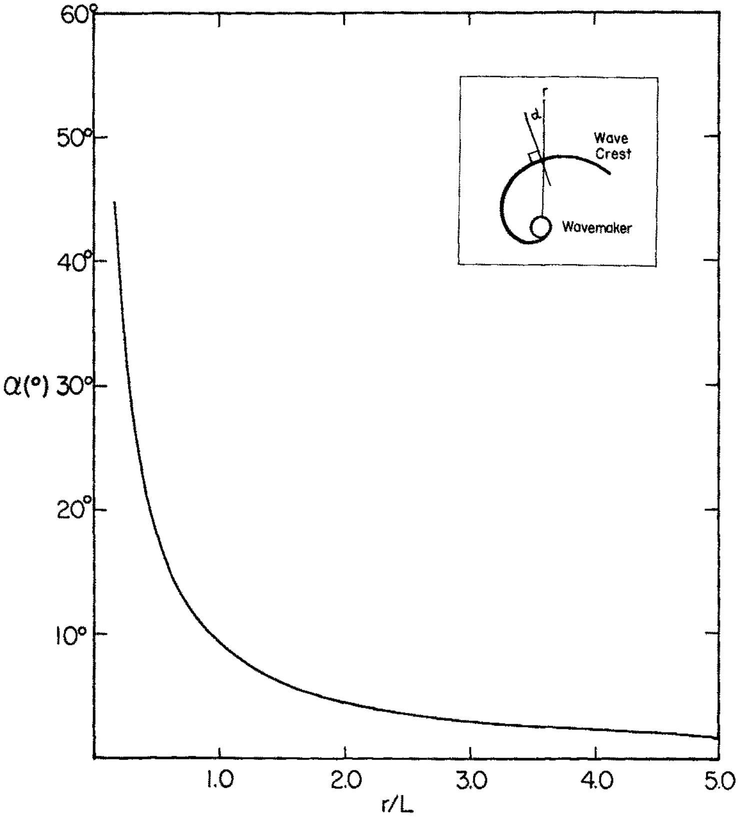

FIGURE 4 ASYMPTOTIC WAVE DIRECTION AS A FUNCTION OF DISTANCE FROM WAVEMAKER

In either case, the power is expressed as

$$P = \rho \frac{|A_o|^2 \sigma}{2k_o} (\sinh 2k_o h + 2k_o h) \tag{21}$$

The dimensionless power for the two cases of wavemaker motion is shown in Figure 5. As expected, the rolling spiral wavemaker (Case 2) is the more efficient wave generator in deep water while in shallow water the converse is true.

Experimental Results

A prototype spiral wavemaker has been constructed and tested against the theory. The wavemaker is composed of a 2' tall, 12.5" diameter steel drum, mounted on an offset shaft which was pulley-driven. The offset of the rotating shaft could be located at either 1" or 2" from the axis of the cylinder. The shaft fit into a floor-mounted bearing and at the top into a cantilevered arm from the electric motor platform. The steel drum was rotated, rather than moved irrotationally, about the axial shaft.

Experimental runs to determine wave heights were conducted in a large 75' x 40' basin filled with 10" of water. The wavemaker was run at different periods to provide a range of relative depths, $k_o h$. Measurements of the spiral wave heights were made at 3' and 9' from the wavemaker and were obtained using a resistance wire gage and recorded by a Hewlett-Packard recorder. The tests were each run twice in succession and independently analyzed by the authors. As an example of the data, see Figures 6 and 7. The tabulated results represent the averaged data for each test. The measured data were then extrapolated to the wavemaker ($r = a$) via the theory, by multiplying by the ratio,

$$\left[\frac{J_1(k_o a)^2 + Y_1(k_o a)^2}{J_1(k_o r_m)^2 + Y_1(k_o r_m)^2}\right]^{\frac{1}{2}}$$

where r_m represents the distance of the wave gage from the wavemaker. The results are also plotted versus the theory in Figure 8. The results are remarkably good for small $k_o h$, particularly in view of the rotational motion of the wavemaker and because of a 3/4" gap between the wavemaker bottom and the floor of the basin. The poor agreement at $k_o h$ greater than 2.0 is attributable to the violations of the conditions of potential flow. For instance, for the $k_o h$ value of 4.55, the wavemaker was rotating at 125 revolutions per minute, and separation occurred behind the cylinder perturbation as it rotated.

Littoral Drift Test

A 16' diameter circular basin was placed around the wavemaker and a fine sand beach was constructed in 9" of water. The wavemaker was operated at a 1 second period and produced waves of approximately 1" in height at the beach.

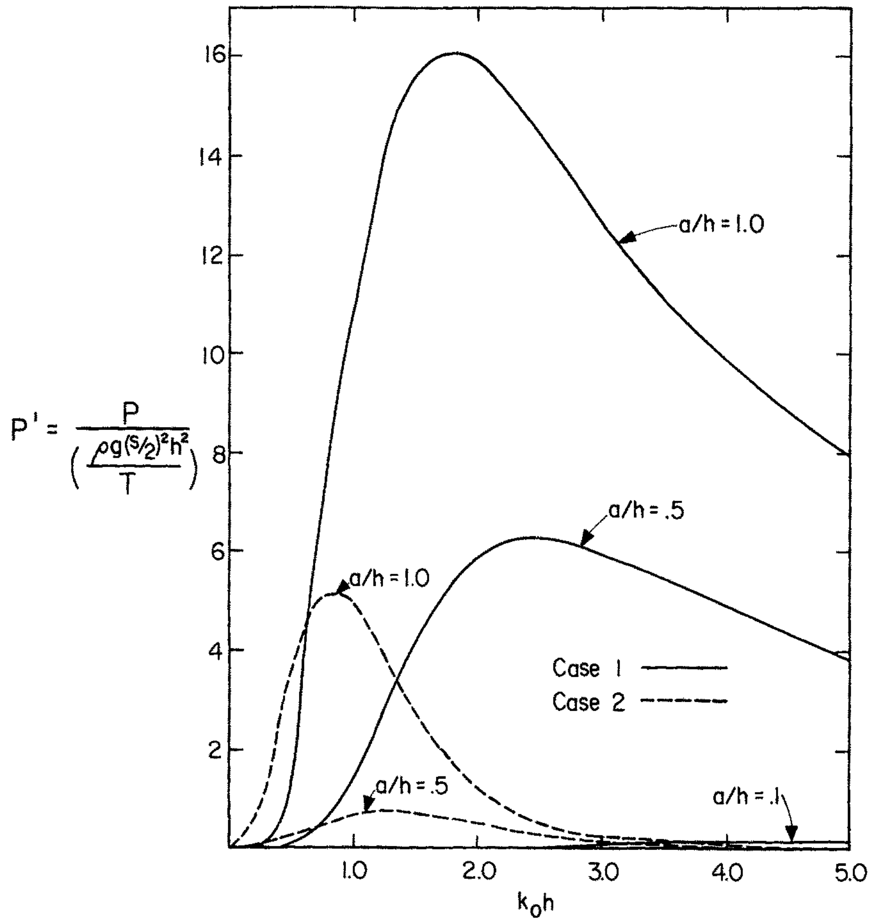

FIGURE 5 DIMENSIONLESS POWER, P', FOR CASES 1 AND 2

EXAMPLES OF TEST DATA

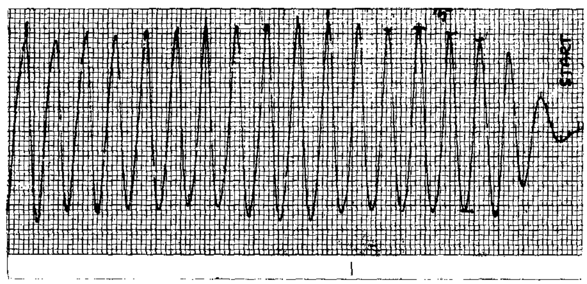

FIGURE 6. Recorded data (3' from wavemaker)
Test Condition: $h = .833'$, $T = .615$ sec, $|\eta|/(S/2) = .667$
$a = .52'$, $(S/2) = 1''$

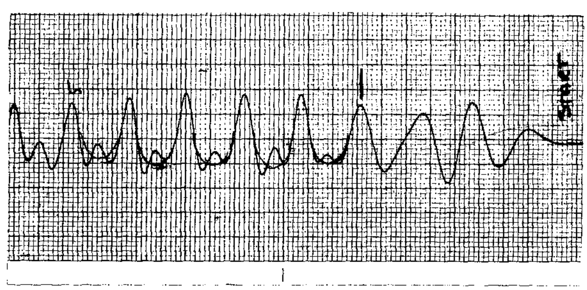

FIGURE 7. Recorded data (9' from wavemaker)
Note presence of first harmonic.
Test Condition: $h = .833'$, $T = 1.18$ sec., $|\eta|/(S/2) = .109$
(not to same scale as above) $a = .52'$, $(S/2) = 1''$.

Table 1. Measured and Predicted Spiral Wave Amplitudes
for Water Depth of 10" and 12.5" Wavemaker Diameter

Wave Period (sec)	Measured Dimensionless Wave Amplitude $\|\eta\|/(S/2)$ at Gage	Distance from Wavemaker (feet)	Dimensionless Wave Amplitude Calculated at Wavemaker from Measured Wave	Predicted Dimensionless Wave Amplitude at Wavemaker	% Error
(S/2)=1"					
1.135	.236	3.0	.690	.748	7.83
1.13	.150	9.0	.766	.760	-7.36
1.61	.055	9.0	.318	.327	2.63
1.55	.108	3.0	.348	.358	2.76
3.11	.0367	3.0	.148	.073	-101.4
2.98	.0087	9.0	.0644	.0805	20.09
3.74	.0068	9.0	.0553	.0494	-12.03
3.82	.0094	3.0	.0402	.0472	14.85
1.19	.213	3.0	.631	.670	5.81
1.18	.109	9.0	.565	.681	16.97
1.99	.0297	9.0	.186	.199	6.35
2.33	.0401	3.0	.147	.140	-6.16
.62	.667	3.0	1.683	1.955	13.90
.48	.479	3.0	1.173	2.041	42.53
.80	.386	3.0	1.025	1.504	31.85
(S/2)=2"					
1.04	.224	3.0	.695	.907	23.36
2.70	.0165	3.0	.0636	.100	36.40
1.405	.130	3.0	.406	.452	10.25

$$* \quad \% \text{ Error} \equiv \frac{\eta_{\text{Predicted}} - \eta_{\text{Measured}}}{\eta_{\text{Predicted}}} \times 100$$

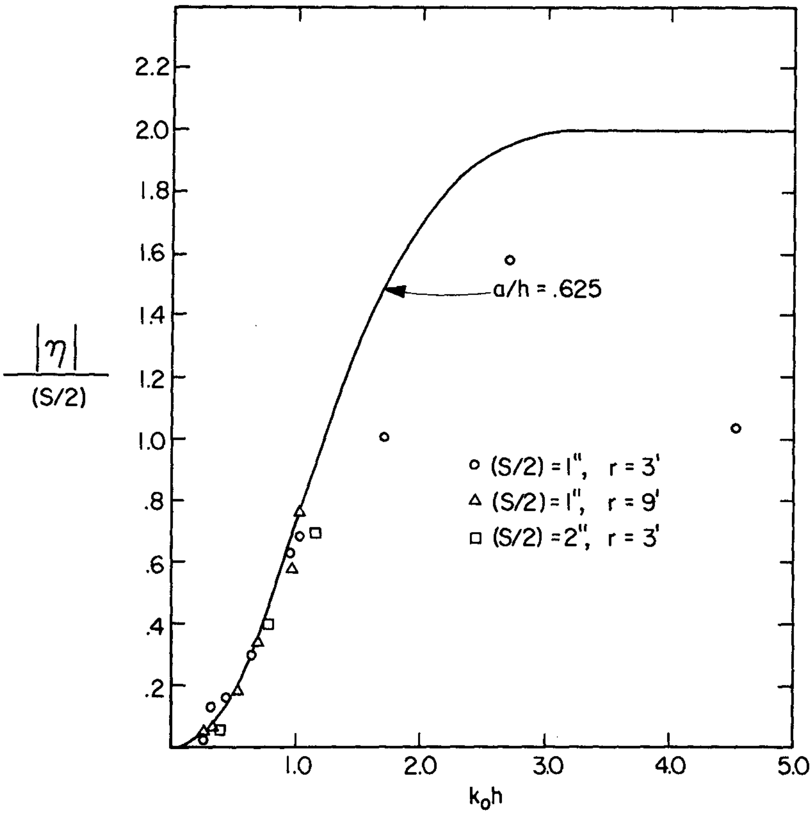

FIGURE 8 THEORETICAL AND EXPERIMENTAL DIMENSIONLESS PROGRESSIVE WAVE AMPLITUDE EVALUATED AT CYLINDER (a= .52') FOR CASE I

Photograph of Spiral Wavemaker With 16' Diameter Circumferential Beach for Littoral Drift Tests. (Cement blocks and sand were removed for wave height measurements).

A steep beach was immediately formed with a shallow foreshore, dropping off at the plunge point of the waves to about 8" in depth. Around the basin, despite obvious reflections due to the beach steepness, a noticeable time lag in wave breaking around the basin was apparent. Fluorescent sand tracer placed in a strip across the foreshore moved readily in the direction of the wavemaker rotation. A rock groin placed across the beach and offshore, showed after two hours of testing, the usual downdrift scour and updrift deposition pattern, despite noticeable leakage of tracer through the groin. After testing, the current attributable to the stirring action of the wavemaker was measured as .05 ft./sec. approximately 2' from the beach, a velocity much lower than the incipient motion velocity of the sand. No qualitative tests were made to determine drift rates.

Conclusions and Recommendations

From this study it is apparent that the spiral wavemaker can be both a practical and a useful research tool for time-dependent littoral drift studies. A much larger spiral wavemaker should be built, in part, to produce large waves and also to keep $\varepsilon(z)/a << 1$; see below. If possible, the wavemaker motion should be irrotational and the clearance between the wavemaker and the basin floor should be a minimum.

The linear spiral wavemaker theory adequately describes the spiral wave for $k_o h < 2.0$. For larger $k_o h$ values separation effects were encountered in these experiments.

The ratio, $\varepsilon(z)/a$, is of importance in the generation of higher wave harmonics. Due to the small but finite displacement of the cylinder from origin, the cylinder wall boundary condition at $r = a$ is in actuality, nonlinear, giving rise to higher harmonics. From geometrical considerations, it can be shown for Case 1 motion that the ratio of the first harmonic amplitude to the fundamental mode is proportional to $\varepsilon(o)/2a$; however, the wave height response to the first harmonic is usually greater due to the increased relative water depth as a result of doubling the angular frequency. In other words, the higher harmonics may be amplified greatly, and therefore the requirement of $\varepsilon(z)/a << 1$ is a strict one. For example, for the data shown in Figure 7, $\varepsilon(z)/2a = .08$; however, the response for the first harmonic is double that of the fundamental, and therefore at the wavemaker, the amplitude of the first harmonic is 16% that of the fundamental wave.

Finally, one possible disadvantage should be emphasized. The angle of the wave to the radial direction of the beach is fixed by the wave period, the water depth, and the distance from the wavemaker. Thus the experimenter does not have a wide range of wave attack angles for littoral drift studies. Should this range be necessary, one possible solution is to change the diameter of the wave basin, or possibly, increase the number of lobes the wavemaker.

Acknowledgement

This work was sponsored, in part, by the NOAA Office of Sea Grant, Department of Commerce, under Grant No. SGP 2-38.

References

1. Biesel, F. and F. Suquet,"Laboratory Wave Generation Apparatus," Proj. Rept. 39, St. Anthony Falls Hydraulic Laboratory, University of Minnesota, Minneapolis, English Translation, 1953.

2. Black, J. L. and C. C. Mei,"Scattering and Radiation of Water Waves," M.I.T., Water Resources and Hydrodynamics Laboratory, Rept. No. 121, April, 1970.

3. Dean, R. G.,"Water Waves Generated by Oscillating Plane and Cylindrical Wavemaker," Unpublished Lecture Notes, University of Hawaii, May 7, 1968.

4. Galvin, C. J., Jr.,"Wave Height Predictions for Wave Generation in Shallow Water," U.S. Army Coastal Engineering Research Center, T.M. 4, 1964.

5. Gilbert, G., D. M. Thompson and A. J. Brewer, "Design Curves for Regular and Random Wave Generations," J. Hyd. Res., IAHR, Vol. 9, No. 2, 1971.

6. Havelock, T. H., "Forced Surface-Waves on Water," Philosophical Magazine, Vol. VIII, Oct. 1929.

7. Krumbein, W. C.,"Shore Currents and Sand Movements on a Model Beach", U. S. Army Beach Erosion Board T.M. 7, Sept., 1944.

8. Saville, T., Jr.,"Model Study of Sand Transport along an Infinitely Straight Beach," Trans. A.G.U., Vol. 31, No. 4, 1950.

9. Ursell, F., R. G. Dean and Y. S. Yu, "Forced Small-Amplitude Water Waves: A Comparison of Theory and Experiment", J. Fluid Mechanics, Vol. 7, Pt. 1, 1960.

10. Yu, Y. S. and F. Ursell, "Surface Waves Generated by an Oscillating Cylinder on Water of Finite Depth: Theory and Experiment, J. Fluid Mech. Vol. 11, 1961.